



A novel hydrogeochemical approach to delineate the origin of potentially toxic elements in groundwater: Sophisticated molar ratios as environmental tracers

Panagiotis Papazotos^{1,2} · Eleni Vasileiou¹ · Stylianos Vasilakis¹ · Maria Perraki¹

Received: 15 December 2022 / Accepted: 14 May 2023 / Published online: 20 May 2023
© The Author(s), under exclusive licence to Springer-Verlag GmbH Germany, part of Springer Nature 2023

Abstract

The occurrence, mobilization, and origin of Potentially Toxic Elements (PTEs) in the environment is always a difficult research question that has not been fully addressed to date; solving this problem would be a major achievement for environmental science and pollution research, a significant scientific breakthrough, and an important contribution to environmental analysis and monitoring. The lack of a holistic methodology that uses chemical analysis to determine the origin of each PTE in the environment is the main motivation for this project. Therefore, the hypothesis tested here is to develop a scientific approach applied to each PTE to determine whether its origin is geogenic (i.e., water-rock interaction with dominance of silicate or carbonate mineral phases) or anthropogenic (i.e., agricultural practices, wastewater, industrial activities). A total of 47 groundwater samples from the Psachna Basin in central Euboea, Greece, were used and plotted on geochemical mole ratio diagrams (i.e., Si/NO₃ vs. Cl/HCO₃) and used to perform a robust geochemical modeling analysis. The proposed method showed that elevated groundwater concentrations of various PTEs in groundwater were mainly related to intensive fertilization (e.g., Cr, U), water-rock interaction (e.g., Ni), and saltwater intrusion (i.e., As, Se). This work highlights that a comprehensive framework with sophisticated molar ratios combined with modern statistical methods, multi-isotope signatures, and geochemical modeling could provide answers to unresolved scientific questions about the origin of PTEs in water resources and improve environmental resilience.

Keywords Euboea · Potentially toxic elements · Fate and transport · Groundwater · PHREEQC · R-mode hierarchical cluster analysis

Introduction

It is generally agreed that geological, environmental, and geochemical factors play an important role in the occurrence, mobilization, transport, and fate of potentially toxic elements (PTEs) in rivers, groundwater, and other streams and waterways (Guo et al. 2014; Papazotos et al. 2020).

The presence of PTEs in the environment, including water supplies, may have been introduced either naturally or by human activities. Various rocks, and consequently the soils/sediments composed of weathering products of source rocks, may be particularly rich in PTEs, as is the case with ultramafic rocks enriched in Cr (Oze et al. 2004), Ni (Kelepertzis et al. 2013), Co (Vithanage et al. 2014), and As (Ryan et al. 2011). However, geochemical conditions have a significant influence on the mobility of PTE in water resources (Kotaś and Stasicka 2000). The Eh/pH system, precipitation/dissolution reactions, sorption, vegetation, and complexation are critical geochemical parameters that need further study in a dynamic and ever-changing system such as groundwater. One question that has preoccupied geoscientists and engineers in recent years is the following: What are the possible natural and anthropogenic sources of PTEs in the groundwater of a study area? (Papazotos 2021). Several integrated and coupled methods have been developed, in particular

Responsible Editor: Xianliang Yi

✉ Panagiotis Papazotos
papazotos@metal.ntua.gr

¹ School of Mining and Metallurgical Engineering, Division of Geo-sciences, National Technical University of Athens, 9 Heroon Polytechniou St, 15773 Zografou, Greece

² School of Engineering, Department of Mineral Resources Engineering, University of Western Macedonia, 50100 Kozani, Greece

Multivariate statistics (i.e., factor analysis using principal component analysis-PCA and hierarchical cluster analysis-HCA methods -Vasileiou et al. 2019; Papazotos et al. 2020), stable multi-isotopic signatures (e.g., $\delta^{53}\text{Cr}$, $^{87}\text{Sr}/^{86}\text{Sr}$, $^{206}\text{Pb}/^{204}\text{Pb}$, $^{207}\text{Pb}/^{204}\text{Pb}$, $^{208}\text{Pb}/^{204}\text{Pb}$, $\delta^{11}\text{B}$, $\delta^{15}\text{N}_{\text{NO}_3}$, and $\delta^{18}\text{O}_{\text{NO}_3}$ - Puig et al. 2017) and machine learning algorithms (e.g., random forest, logistic regression, support vector machine, artificial neural network, bagging, etc.. - Ruidas et al. 2021; Ruidas et al. 2022; Egbueri and Agbasi 2022) are widely used to determine the origin of PTEs in groundwater. However, there is currently no methodological framework that can definitively determine the origin of each PTE based on the specific geochemical characteristics that determine its concentration in natural waters.

In addition to the approaches described above, the calculation of ionic ratios is an important technique for evaluating geochemical processes in the aquifer and provides useful information about hydrogeochemistry and the origin of solutes. Among the different ion ratios, Na/Cl , Cl/HCO_3 , Mg/Ca , Na/Ca , Cl/SO_4 , $(\text{Ca}+\text{Mg})/(\text{HCO}_3+\text{SO}_4)$, Cl/NO_3 are the most commonly used and are mainly used for a deeper understanding of the main geochemical processes such as salinization (Abdalla 2016; Alcalá and Custodio 2008), ion exchange (Abdalla 2016), water-rock interaction (Papazotos et al. 2020), and N-cycle processes (Chen et al. 2009). More specifically, higher or lower Cl/HCO_3 values indicate groundwater salinization due to saltwater intrusion or freshwater recharge, respectively (Revelle 1941). Alternative ion ratios such as Cl/NO_3 are used to distinguish the source of N in water resources; higher Cl/NO_3 values could indicate input from manure or/and sewage input, while lower Cl/NO_3 values could indicate N-containing or mixed fertilizers as the main source of NO_3^- in an aquifer (Chen et al. 2009). However, the use of ionic ratios is limited to studying the extent of saltwater intrusion or freshwater recharge in an aquifer, although it would be very interesting to use them to evaluate the presence of PTEs in groundwater. Another limitation is that the studies using ionic ratios refer only to the chemistry of major ions, while trace elements have been used in only a few studies. For example, Alcalá and Custodio (2008) found that Cl/Br molar ratio is a reliable tracer for determining the source of groundwater salinity. Therefore, trace element dynamics in an ionic ratio approach involving more than one ionic ratio could reveal hidden trends indicative of the origin of PTEs in groundwater, a method that is not yet widely used but whose application could be an important additional tool for delineating important contaminants.

Since 2010, elevated groundwater concentrations of PTEs, particularly Cr, have been reported in the Psachna basin, central Euboea, Greece (Megremi 2010). These concentrations have been attributed to both natural sources, such as dissolution of ultramafic rocks (Papazotos et al. 2019), and anthropogenic influences, such as intensive overfertilization

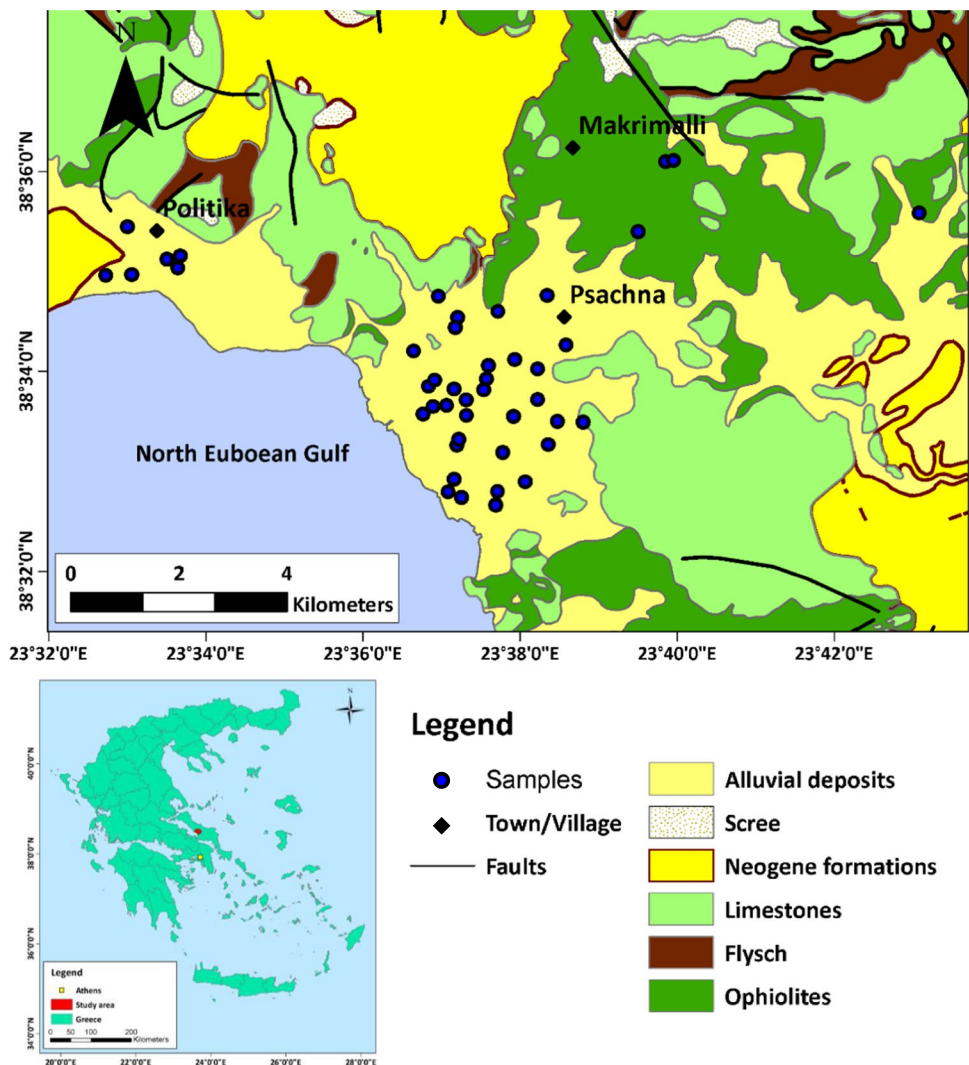
(Remoundaki et al. 2016; Papazotos et al. 2019) and salt-water intrusion (Remoundaki et al. 2016; Eliopoulos et al. 2021). The source of PTEs in Psachna Basin groundwater has been determined using multivariate statistical analyses (i.e., factor analysis and HCA) (Megremi et al. 2019; Papazotos et al. 2019) and stable isotope signatures of ^{53}Cr (Economou-Eliopoulos et al. 2014; 2017). However, these widely used techniques have their limitations, highlighting the need to develop a holistic methodology that uses chemical analyses to separate anthropogenic and geogenic factors for each PTE. Although numerous geochemical studies have been carried out, holistic geochemical modelling, including calculation of ionic ratios, has yet to be conducted.

The aim of this research is to: a) develop a comprehensive methodology that can be used for any PTE to determine whether it is of natural or anthropogenic origin, and b) analyze the occurrence and mobility of PTEs using advanced geochemical modeling tools. For the first time, a) ion ratios are linked to generate innovative hydrogeochemical diagrams to determine the origin of PTEs in groundwater, and b) real mineralogical data are evaluated for their potential contribution PTE using PHREEQC geochemical modeling software. The main objective of this study is to develop a complete approach that can be used for most PTEs and in any geologic setting, providing the scientific community with important insight into the complicated - and to date not fully understood - issue of the occurrence and mobilization of PTEs in the environment. This approach is being applied in the widely studied ultramafic area of the Psachna Basin, where both geogenic and anthropogenic influences are believed to contribute to the elevated concentrations of PTE in groundwater. The results of this research will be important for environmental scientists and policy makers to determine the exact source of each PTE in the environment and improve environmental and societal resilience as it will impact several important aspects such as science, environment, and human health.

Case study

The Psachna Basin is located on the island of Euboea in Greece at coordinates $38^\circ 32' 00''$ – $38^\circ 36' 28''$ N (latitude); $23^\circ 32' 00''$ – $23^\circ 43' 00''$ E (longitude). (Figure 1); The town of Psachna is located about 90 km from Athens, Greece. Forests and farmland make up most of the basin's area, closely followed by olive trees. Cereals, horticultural crops, olive groves, legumes, carrots, potatoes, cabbage, lettuce and broccoli are the main products of the current intensive agricultural activity. According to Köppen's climate classification, the Psachna Basin has a typical semi-arid Mediterranean climate (C_{sa}) characterized by cold, rainy winters and hot, dry summers (Köppen 1931).

Fig. 1 A simplified geological map of the study area (after Katsikatsos et al. 1981) and sampling sites.



This area includes a wide range of rocks, from ultramafic (i.e., serpentinites and peridotites) to mafic (i.e., diabase) rocks and sediments of Quaternary and Neogene age to Cretaceous carbonate formations (limestones and dolostones), and Fe-Ni ore deposits (Katsikatsos et al. 1981). The studied alluvial aquifer is located in the lowlands of the basin and developed in Quaternary sediments; it consists of ultramafic rocks and limestones eroded over a total area of 21 km². Precipitation, infiltration of surface runoff (torrents), and lateral inflows from groundwater systems formed in carbonate and fractured ultramafic rocks in the northern part of the basin contribute to natural groundwater recharge (Dandolos and Zorapas 2010). The groundwater flow direction is from the northeast to the southwest and the alluvial aquifer system has a hydraulic conductivity of about 2 x 10⁻⁴ m/s.

Materials and Methods

The methodology of this work includes the following steps: i) groundwater sampling, ii) analytical determination of physical and chemical parameters using different techniques, iii) data set preparation, iv) mineralogical identification, and v) geochemical modeling using PHREEQC software. Further information on each phase is provided in the following subsections.

Sampling

A total of 47 groundwater samples were collected from irrigation wells to assess groundwater quality in the

Psachna Basin (Fig. 1); this work includes 33 groundwater samples from Papazotos et al. (2019) and 14 new groundwater samples from a sampling campaign conducted in October 2019 (Vasilakis et al. 2022). Finally, the final dataset includes four seasonal sampling campaigns: the first in December 2016, the second in June 2017, the third in November 2017, and the fourth in October 2019. All samples from irrigation wells were collected by pumping for a sufficient period of time (at least 15 minutes) to flush out all residual water volume. Water samples were collected in 1000-mL polyethylene bottles that had been pre-cleaned, acid washed, and thoroughly rinsed first with distilled water and then with deionized Milli-Q water. The polyethylene bottles were rinsed three times with the water to be sampled before collection. During sampling, samples were stored in a portable cooler with cold packs and refrigerated at 4° C until chemical determination.

Determinations

Physical parameters

Immediately after sampling, the physical parameters of electrical conductivity (EC), dissolved oxygen (DO), pH, and Eh were measured in situ using the YSI Professional Digital Sampling System (ProDSS) (Xylem, USA). The total dissolved solids (TDS) parameter was also calculated by summing the major ions.

Chemical parameters

Each sample of 1000 mL was separated into three different subsamples for a different chemical determination; one of 500 mL to determine major ions (i.e., Ca^{2+} , Mg^{2+} , Na^+ , K^+ , Cl^- , SO_4^{2-} , HCO_3^- , NO_3^- , NO_2^- , and NH_4^+), one of 100 mL to determine PTEs and other trace elements (i.e., As, B, Ba, Br, Cd, Co, Cr, Cu, Mn, Mo, Ni, P, Pb, Rb, Sb, Se, Si, Sr, U, V, and Zn) after filtering through a 0.45 μm filter and acidifying with 1M HNO_3 , and one of 25 mL to determine Cr(VI) by ion exchange using IC-All tech cartridges (Ball and McCleskey 2003), after filtering through 0.45- μm and acidifying with 1M HNO_3 . Table 1 provides an overview of

the analytical methods for calculating physical and chemical parameters. Within 8 hours of the sampling, the 500-mL subsamples were transported right away to the lab where, before any analysis or additional processing, the subsamples were passed through 0.45 μm filters. None of the 500-mL samples exhibited any significant turbidity. All the samples were kept at 3–7°C, but each parameter received a different treatment: a) Ca^{2+} , Mg^{2+} , Na^+ , and K^+ were acidified to a pH of 2 with 1 M HNO_3 , and their analyses were completed within 10 days; b) NO_3^- and HCO_3^- were completed within 24 hours; and c) Cl^- and SO_4^{2-} were completed within 10 days. The above procedures were in accordance with the American Water Works Association (AWWA)/American Public Health Association (APHA)/Water Environment Federation Standard Methods for the Examination of Water and Wastewater (WEF) recommendations. The analyses used the international quality control (QC) and quality assurance (QA) protocols (including blanks, QC standards, and QC samples).

Inductively coupled plasma mass spectrometry (ICP-MS) was used to measure PTEs and other trace elements at the analytical laboratories of Bureau Veritas Commodities Canada Ltd. in Vancouver, British Columbia, while a ICP-MS Agilent Technologies 7700 series was used to determine Cr(VI) at the National Technical University of Athens, Greece. Analyses were performed within seven days following APHA standard procedures (APHA 2012). The Bureau Veritas Commodities Canada Ltd. laboratory is accredited to the ISO /IEC 17025:2005 standard, which includes both QC and QA protocols. The field and laboratory composite samples and duplicate sample analyses were part of the QC processes.

Data processing

ESRI's ArcGIS v.10.3 program was used to create a geologic map to visualize the study sampling locations. The software IBM SPSS v.22 was used to perform the statistics. Data processing included: i) data validation, ii) descriptive statistical analysis, iii) Spearman rank correlation coefficients, and iv) HCA in R mode. The descriptive statistical analysis includes the mean, minimum (min), maximum (max), and median

Table 1 The analytical techniques of each determined parameter.

Parameter	Analytical technique
EC, DO, pH, Eh	YSI Professional Digital Sampling System (ProDSS)
Ca^{2+} , Mg^{2+} , Na^+ , K^+	Atomic absorption spectrometry (AAS)
NO_3^- , NO_2^- , NH_4^+	Spectrophotometry
Cl^- , HCO_3^-	Titrimetry
SO_4^{2-}	Turbidimetry
As, B, Ba, Br, Cd, Co, Cr, Cr(VI), Cu, Mn, Mo, Ni, P, Pb, Rb, Sb, Se, Si, Sr, U, V, and Zn	Inductively coupled plasma mass spectrometry (ICP-MS)

values, standard deviation (SD), first quartile (Q1), and third quartile (Q3). For statistical analysis, the values below the detection limit (BDL) of the analysis method were set to the value of the detection limit (DL). The mean, median and SD values of a parameter that occurred in more than 50% of the samples BDL were not calculated (NC).

Due to the small sample size, data outliers were included in the correlation analysis to determine the relationship between the two parameters; however, the use of the non-parametric robust Spearman rank correlation coefficient (r) reduced the weighting of the potential influence of the outliers (Filzmoser et al. 2018). Equation (1) (Spearman 1904) is used to calculate the Spearman rank correlation coefficient:

$$r_s = 1 - \frac{6 \sum_{i=1}^n d_i^2}{n(n^2 - 1)} \quad (1)$$

Where d_i = difference in paired ranks, n = number of cases, x_i and y_i = data pair.

The formula to use when there are tied ranks is (2):

$$\rho = \frac{\sum_i (x_i - \bar{x})(y_i - \bar{y})}{\sqrt{\sum_i (x_i - \bar{x})^2 \sum_i (y_i - \bar{y})^2}} \quad (2)$$

The magnitude of the absolute value (from better to worse association) was used to divide the correlation coefficient values, which ranged from 1 to 1, into five equally sized groups: very strong (0.8-1), strong (0.6-0.79), moderate (0.4-0.59), weak (0.2-0.39), and very weak (0-0.19). (Evans 1996). The correlation coefficient is considered highly statistically significant, marginally statistically significant, and not statistically significant if the p value is $p < 0.01$, $p < 0.05$, and $p > 0.10$, respectively.

Hierarchical cluster analysis (HCA) is an algorithmic multivariate statistical analysis method for grouping individuals with similar characteristics. In hydrogeochemical studies, HCA classification is used to group samples (Q-mode) or parameters (R-mode) into clusters based on their (dis)similarity, resulting in a tree diagram, also known as a dendrogram. The focus of this study was on the relationship between the studied parameters, so HCA was performed in R-mode using Ward's (1963) method as the linkage and squared Euclidean distances as the similarity measure.

Mineralogy

A detailed geochemical, petrological, and mineralogical study of the rocks and soils was performed using optical microscopy, X-ray diffraction analysis (XRD; Bruker D-8 Focus), and scanning electron microscopy (SEM; JEOL6380LV). About 10 g of the sample was ground in a

mechanical mill to determine the qualitative mineralogical composition by XRD. XRD analysis was performed at 2 θ from 2 $^\circ$ to 72 $^\circ$ with CuK α radiation ($\lambda=1.5405 \text{ \AA}$) and Ni filter at 40 kV and 30 mA. Mineral phases were identified based on characteristic hkl reflectance distances using EVA version 12 software.

Geochemical modeling

The saturation index (SI) with respect to mineral phases was calculated using the PHREEQC geochemical program (Parkhurst and Appelo 1999), with MINTEQA4 serving as the primary thermodynamic database to evaluate chemical reactions in groundwater (Allison et al. 1991). Hydrogeochemistry is controlled by the interaction of water with rocks and soil, and geochemical software was used to provide the SI of specific mineral phases found in the study area. The SI of the water samples can be defined by the following equation (3):

$$SI = \log \left(\frac{IAP}{K_{sp}} \right) \quad (3)$$

where IAP is the Ion Activity product and K_{sp} is the equilibrium constant.

When the SI value is equal to 0, the solution is in equilibrium with the mineral phase; when the SI value is > 0 , the solution is oversaturated, resulting in mineral precipitation, and when the SI value is < 0 , the solution is undersaturated indicating that dissolution is required to reach equilibrium.

Results

Chemometrics

The analytical accuracy of the ion measurement was determined to be less than $\pm 10\%$ by calculating the charge balance error in each sample. The descriptive statistics for a total of 39 physical and chemical parameters of the 47 groundwater samples from the Psachna Basin are presented in Table 2. The most interesting physical parameters for the field of environmental geochemistry are pH and Eh, which ranged from 7.21 to 8.86 and from 136 mV to 331 mV, respectively. On the other hand, remarkable NO_3 (up to 540 mg/L) and PTE groundwater concentrations were determined (up to 162 $\mu\text{g/L}$ Cr; up to 5.12 $\mu\text{g/L}$ U; up to 21.1 $\mu\text{g/L}$ Ni; up to 610 $\mu\text{g/L}$ Zn; up to 3.3 $\mu\text{g/L}$ As; up to 6.9 $\mu\text{g/L}$ V; up to 5.2 $\mu\text{g/L}$ Se). Furthermore, an additional parameter was calculated to further investigate the total PTEs (TPTEs) load in groundwater by summing selected PTEs; therefore, this parameter

Table 2 Descriptive statistics (mean, min, max, median, standard deviation, 1st Quartile, and 3rd Quartile) of the physical and chemical parameters for the 47 analyzed groundwater samples from the Psachna Basin.

Parameter	Unit	DL	Mean	Min	Max	Median	SD	Q1	Q3
DO	mg/L	-	7.58	3.43	12.8	7.8	1.69	6.69	8.67
EC	μS/cm	-	1149	334	2763	1062	436	909	1334
TDS	mg/L	-	835	207	1773	791	298	659	943
pH	-	-	7.72	7.21	8.86	7.61	0.37	7.50	7.85
Eh	mV	-	265	136	331	278	38.4	254	288
Ca ²⁺	mg/L	0.2	91.2	4.48	150	91.9	29.5	75.1	110
Mg ²⁺	mg/L	1	78.6	32.2	216	69	34.5	59.1	87.4
Na ⁺	mg/L	2	42.2	9.3	156	36.4	24.1	30.5	48
K ⁺	mg/L	0.2	2.85	0.57	26.2	1.76	3.88	1.3	2.94
NO ₃ ⁻	mg/L	1	136	4.7	540	106	110	54.6	180
NO ₂ ⁻	mg/L	0.05	NC	BDL	19	NC	NC	BDL	0.1
NH ₄ ⁺	mg/L	0.05	NC	BDL	0.12	NC	NC	BDL	BDL
Cl ⁻	mg/L	5	84.2	15	396	66	72.8	44	96
SO ₄ ²⁻	mg/L	5	85	5	310	78	61.5	35.5	118
HCO ₃ ⁻	mg/L	10	315	129	598	312	89.9	252	355
Al	μg/L	1	NC	BDL	19	NC	NC	BDL	2
As	μg/L	0.5	1.01	BDL	3.3	0.8	0.56	0.6	1.2
B	μg/L	5	45.2	11	123	35	26.1	27	61
Ba	μg/L	0.05	54	3.17	197	51.4	37.8	33.3	66.2
Br	μg/L	5	368	73	1785	323	309	182	407
Cd	μg/L	0.05	0.05	BDL	0.1	NC	NC	BDL	BDL
Co	μg/L	0.02	0.13	BDL	0.5	0.09	0.12	0.06	0.14
Cr	μg/L	0.5	71.1	4	162	75	34.9	46.5	87.9
Cr(VI)	μg/L	0.5	57.4	4	131	58.7	29.4	35.1	73.1
Cu	μg/L	0.1	2.82	0.2	35.5	2.1	5.05	1.15	2.8
Fe	μg/L	10	NC	BDL	14	NC	NC	BDL	BDL
Li	μg/L	0.1	6.21	1	22.5	5.2	4.38	3.9	6.75
Mn	μg/L	0.05	2.5	BDL	25.5	0.95	4.51	0.54	2.26
Mo	μg/L	0.1	0.19	BDL	1.1	0.2	0.16	BDL	0.2
Ni	μg/L	0.2	4.86	0.7	21.1	3.9	3.42	3.1	6.9
P	μg/L	10	29.5	10	107	26	19	15.5	34.5
Pb	μg/L	0.2	0.46	BDL	2.2	0.3	0.44	BDL	0.55
Rb	μg/L	0.01	0.58	0.07	1.93	0.51	0.33	0.36	0.81
Se	μg/L	0.5	1.42	BDL	5.2	1.2	1.02	0.7	1.6
Si	μg/L	40	16101	4069	41954	15616	6070	13481	18325
Sr	μg/L	0.01	327	29.4	813	329	172	233	410
U	μg/L	0.02	1.98	0.03	5.12	1.86	1.48	0.44	3.02
V	μg/L	0.2	2.44	0.4	6.9	2.3	1.32	1.65	2.7
Zn	μg/L	0.5	70.3	0.7	610	26.7	116	7.5	84.8
TPTEs	μg/L	-	157	23.6	690	139	114	91	181

DL: Detection Limit

SD: Standard Deviation

Q1: First Quartile

Q3: Third Quartile

NC: Not Calculated

BDL: Below the Detection Limit

quantifies the total amount of potentially toxic elements in groundwater and is referred to as TPTEs in the text. The selected PTEs were As, Cd, Co, Cr, Cu, Mn, Ni, Pb, Se, U, and Zn and were chosen based on their importance

in terms of their reference abundance in relevant studies (Papazotos 2021) and their toxicity to living organisms. TPTE values range from 23.6 μg/L to 690 μg/L, with a mean value of 157 μg/L (Table 2).

Table 3 Spearman rank correlation matrix and correlation significance (p values) of selected physical and chemical parameters of the groundwater samples of the Psachna Basin (N = 47). Color repre-

sents the classification of the absolute correlation value between two parameters i.e., Red:0.80-1.00, Orange: 0.60-0.79, Yellow: 0.40-0.59, Blue: 0.20-0.39, and Green: 0.00-0.19.

Table with 31 columns (DO, EC, TDS, pH, Eh, Ca2+, Mg2+, Na+, K+, NO3-, Cl-, SO42-, HCO3-, As, B, Ba, Br, Co, Cr, Cu, Li, Mn, Ni, P, Rb, Se, Si, Sr, U, V, Zn) and 31 rows (DO, EC, TDS, pH, Eh, Ca2+, Mg2+, Na+, K+, NO3-, Cl-, SO42-, HCO3-, As, B, Ba, Br, Co, Cr, Cu, Li, Mn, Ni, P, Rb, Se, Si, Sr, U, V, Zn). The cells contain correlation coefficients and significance values, with some cells highlighted in red, orange, yellow, blue, or green.

Spearman rank correlation coefficients

The Spearman rank correlation matrix of 47 groundwater samples of the Psachna Basin is presented in Table 3. The autocorrelation is not highlighted in red in Table 3, because it is always equal to 1.

R-mode HCA

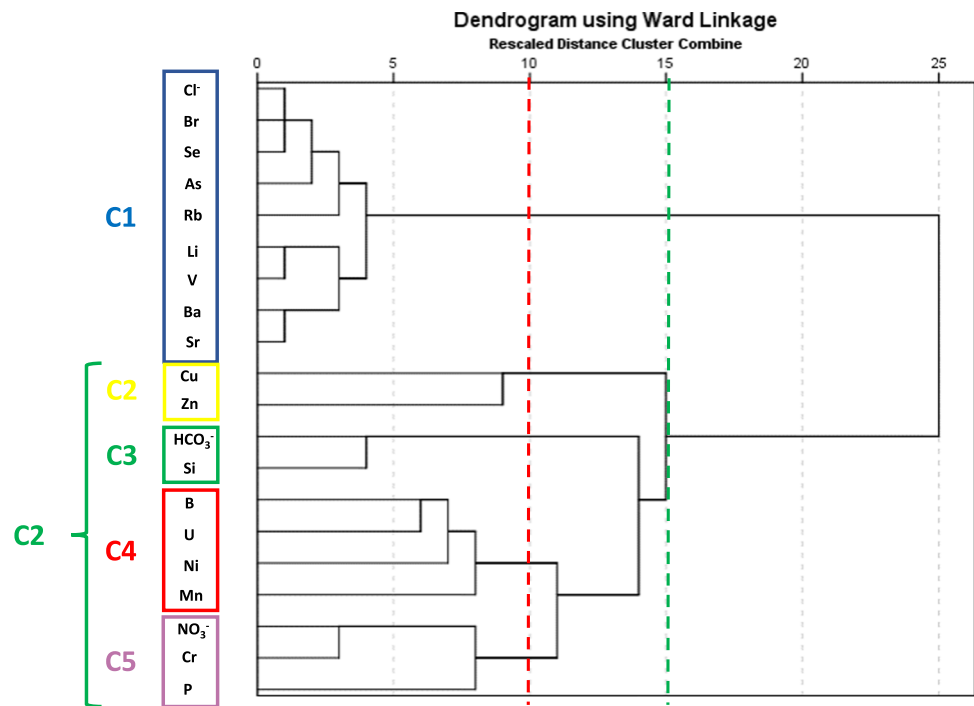
R-mode HCA was conducted to classify group-related hydrochemical parameters, reveal hidden relationships among chemical parameters, and further evaluate processes associated with elevated groundwater PTEs and other trace element concentrations in the Psachna Basin. In this approach, major ions that provide clear evidence of the origin of PTEs (i.e., Cl-, Si, NO3-, HCO3-) were included; those with multifactorial origins (i.e., Ca2+, Mg2+, SO42-, etc.; Papazotos et al. 2019) were excluded. Multivariate statistical analyses such as factor analysis (Voutsis et al. 2015; Papazotos et al. 2019; Megremi et al. 2019) and Q-mode HCA (Voutsis et al. 2015; Papazotos et al. 2019) were performed in the study area. However, R-mode HCA focusing on a large dataset of PTEs has yet to be performed. Parameters with a linkage distance of less than ten (red dashed line; Fig. 2) and about 15 (green dashed line; Fig. 2) were grouped in the same cluster to form different parameter groups with similar hydrogeochemical patterns. As shown in the dendrogram (Fig. 2), the parameters were divided into five main clusters

at the lower coupling distance and two main clusters at the higher coupling distance. The relationship between the two approaches is that cluster 2 of the green dashed line contains clusters 2-5 of the red dashed classification, indicating their hydrogeochemical proximity.

Mineralogy

The predominant lithologic types in the study area are ultramafic rocks, mainly serpentinites and partially serpentinized peridotites, in which the original mineralogical and histological features are still preserved (Fig. 3). Other ultramafic rocks such as harzburgites, dunites, and lherzolites also occur in the wider area. The major mineralogical phase of the dunites is forsterite, while enstatite occurs only in minor amounts (< 5%). Harzburgites consist of forsterite and enstatite (MgO = 34.6-35.75% w/w and FeO = 4.8-5.9% w/w) in proportions of 80-90% and 10-20%, respectively. Diopside (up to 1.5 % v/v) grows mainly in the cleavage of enstatite, forms lamellae and occurs less frequently as small single crystals. Chromium-rich spinel (Cr2O3 = 37 to 55% w/w) usually forms euhedral crystals. The total Fe content of the chromites of Euboea varies between 14 and 20% w/w. Mineralogical phases such as quartz, calcite, illite, kaolinite, montmorillonite, nontronite, chlorite, serpentine, goethite, hematite, and Mn oxides were detected in the soils of the wider study area (Megremi et al. 2019; Economou-Eliopoulos et al. 2014). The Cr2O3 was detected in mineralogical

Fig. 2 Dendrogram in R-mode HCA for 20 parameters determined in groundwater samples from a total of 47 water samples from the Psachna Basin. The red and green dashed line represents the linkage distance used to create different distinct clusters.



phases of ultramafic rocks such as spinel (30–55 wt%), pyroxene (enstatite from 0.2 to 0.5 wt% and diopside from 0.3 to 0.97 wt%), amphibole (0.2–0.7 wt%), serpentine (0.2–0.6 wt% with decrease in Cr_2O_3 content from the core to the edge of the crystal), rarely talc (0.3–0.4 wt%) and chlorite (1.1–2.4 wt%), indicating its geogenic occurrence in the rocks of the area (Megremi et al. 2019; Vasileiou et al. 2014). In the laterites of the area, the main Cr_2O_3 mineral is chromite, which has an inhomogeneous composition with a variation of $\text{Cr}/(\text{Cr} + \text{Al})$ from 0.4 to 0.79. Another important Cr-bearing mineral is the pisolitic goethite of the ore with an average Cr_2O_3 content of 0.89% (w/w), while a small percentage of Cr_2O_3 (0.7% w/w) is present in Ni-chlorite (Megremi et al. 2019). Significant Cr-bearing mineral phases in soils are spinels (chromite, magnetite) (29–61% w/w), Ni-chlorite (up to 0.83% w/w), and goethite (up to 1.34% w/w) (Megremi et al. 2019).

Geochemical modeling

Table 4 summarizes the mineralogical phases identified in the Psachna Basin and provides information for the calculated SIs of the 47 groundwater samples. The major Cr-bearing mineral phases found in the unsaturated state were minerals of the serpentine subgroup (such as lizardite and chrysotile), pyroxene (enstatite and diopside), chlorite, illite, and forsterite, while oversaturated mineral phases were chromite, magnetite, talc, Fe-(hydro)oxides, and so on.

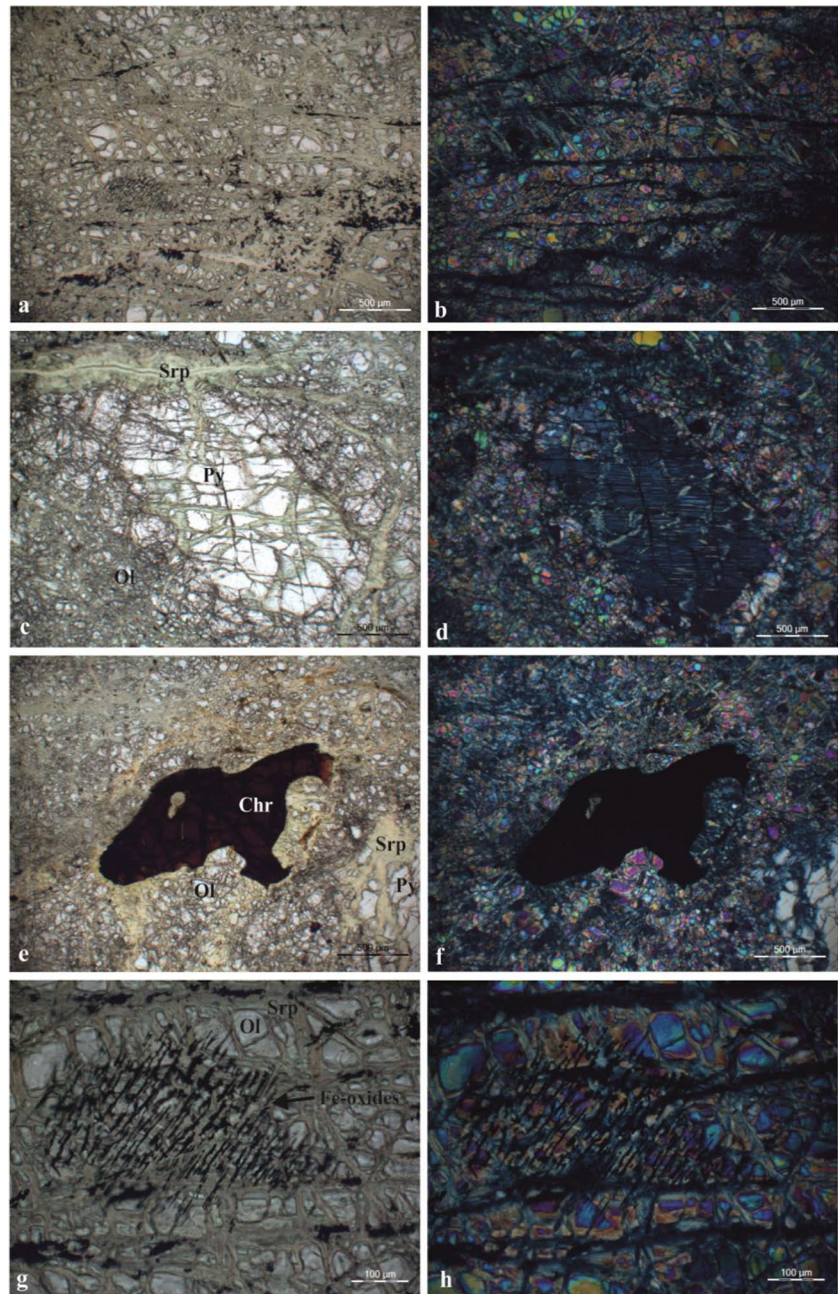
Discussion

PTEs load in the aquifer

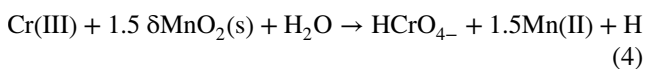
According to the plot of TPTEs versus (vs.) pH values in the modified Ficklin diagram, the total load of selected PTEs in groundwater of the Psachna Basin is generally low (Fig. 4; Ficklin 1992). The prevailing near-neutral to slightly alkaline pH (from 7.21 to 8.86) is the key factor preventing mobilization of cationic PTEs in groundwater (i.e., Pb, Cd, Cu, Ni, Co) (Hermann and Neumann-Mahlkau 1985), which account for the majority of PTEs studied here.

As for the hydrogeochemistry of the study area, Cr is the most important PTE, since it has the highest concentration of all PTEs (Fig. 5). In general, the geochemistry of Cr is very interesting because it is able to change its valence state in the environment both geogenically (i.e., in the presence of Mn oxides, Fendorf et al. 1992) and anthropogenically (i.e., as a NO_2/NO_3 oxidant, Mills and Goldhaber 2012; Papazotos et al. 2019). Trivalent Cr mainly forms trivalent cations or hydrolysates, which usually form metal hydroxide precipitates with low solubility and low mobility, while Cr(VI) is usually in the form of chromate anions (i.e., CrO_4^{2-}) with high mobility (Richard and Bourg 1991). Cr(VI) is the predominant form of Cr in groundwater of the Psachna Basin; (Papazotos et al. 2019). Finally, the pH-Eh diagrams for Mn (Pourbaix 1966) showed that Mn(II) dominates in the groundwater samples of the Psachna Basin (Papazotos et al. 2019b),

Fig. 3 Photomicrographs of serpentinised harzburgites. Residual forsterite and enstatite crystals are distinguished in a matrix of serpentine, Fe-oxides, and chromite granules. In addition, diopside was developed in the cleavage of enstatite (Srp: serpentine, Ol: olivine/forsterite, Py: pyroxene, Chr: chromite, Fe-oxides: iron oxides).



confirming that the natural oxidation reaction (Rai et al. 1987; Richard and Bourq 1991) proceeds according to equation (4):



The dominance of Cr(VI) species and their elevated groundwater concentrations make Cr a PTE of concern, especially in Cr-rich environments such as ultramafic-dominated areas.

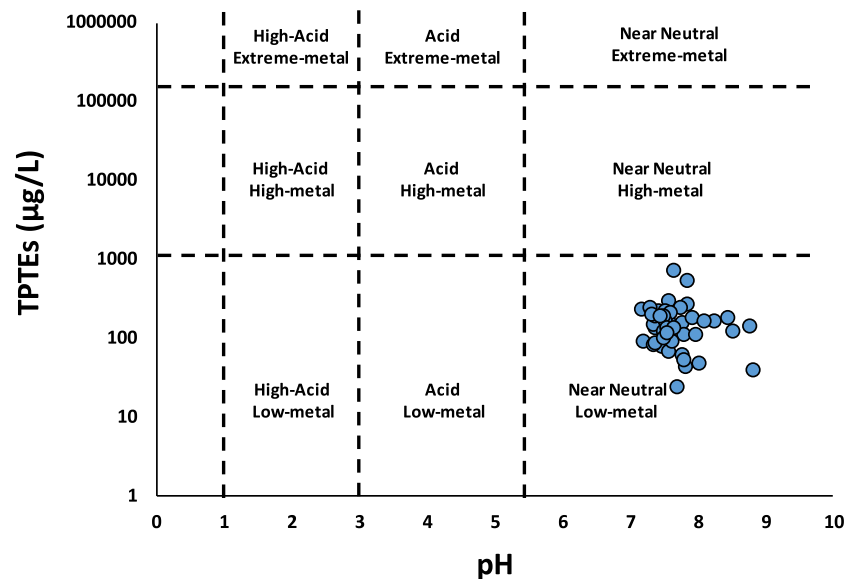
It is worth noting that Zn concentrations are not negligible, but have a wide range of variation. In general, Zn is

considered one of the most mobile PTEs in natural waters, because it forms soluble compounds at neutral and acidic pH, while - at higher pH - Zn can form carbonate and hydroxide complexes that control Zn solubility (Małeck et al. 2017). The remaining PTEs have a small contribution to the total PTE concentration, but some of them (Cd, Cu, Mn, Ni, and Pb) have upper outliers, suggesting that the prevalence of certain geochemical conditions is responsible for elevated groundwater concentrations in some samples. This work, compared to the study of papazotos et al. (2019), utilizes the whole dataset of PTEs and emphasizes creating a methodological framework for delineating their origin in groundwater.

Table 4 Descriptive statistics (mean, min, max, median, standard deviation, 1st Quartile, and 3rd Quartile) of the SIs of the examined mineral phases for the 47 analyzed groundwater samples from the Psachna Basin.

Mineral phase	Mean	Min	Max	Median	SD	Q1	Q3
Lizardite	-2.08	-5.16	3.85	-2.76	2.06	-3.25	-1.48
Chrysotile	-1.46	-4.54	4.47	-2.14	2.06	-2.63	-0.86
Enstatite	-2.80	-3.81	-0.97	-3.04	0.68	-3.25	-2.54
Diopside	-3.83	-5.71	-0.03	-4.27	1.29	-4.60	-3.40
Chlorite(14A)	-0.55	-5.18	8.52	-1.64	3.22	-2.70	0.50
Feldspar	-1.86	-3.63	-0.27	-1.89	0.69	-2.18	-1.53
Quartz	0.39	-0.22	0.84	0.42	0.19	0.35	0.48
Chromite	13.19	10.20	16.46	13.25	0.98	12.79	13.64
Magnetite	13.23	12.32	16.18	13.11	0.71	12.84	13.39
Goethite	4.78	4.22	5.21	4.76	0.21	4.64	4.91
Illite	-1.64	-4.24	1.56	-1.80	1.10	-2.08	-1.12
Talc	2.12	-0.89	7.42	1.43	2.03	0.82	2.96
Brucite	-4.19	-5.24	-1.81	-4.37	0.72	-4.62	-4.01
Forsterite	-6.91	-8.97	-2.75	-7.37	1.39	-7.68	-6.51
Anorthite	-5.01	-6.48	-2.68	-5.25	0.85	-5.48	-4.85
Calcite	0.51	-0.63	1.44	0.44	0.33	0.35	0.63
K-mica	2.96	0.17	7.06	2.69	1.32	2.40	3.46
Kaolinite	0.75	-1.99	3.43	0.74	0.96	0.30	1.12
Montmorillonite	-0.22	-2.94	2.09	-0.27	0.97	-0.51	0.21
Hematite	11.96	10.84	12.83	11.91	0.41	11.69	12.22
Birnessite	-11.64	-14.53	-4.73	-11.78	2.13	-13.05	-10.99
Pyrolusite	-9.58	-12.47	-2.67	-9.72	2.13	-10.99	-8.93

Fig. 4 Ficklin diagram (Ficklin 1992) of the 47 groundwater samples of the Psachna Basin.



The importance of analyzing dissolved Si in groundwater

It is assumed that the dissolved Si in groundwater originates solely from the interaction between water and rock (i.e., anthropogenic activities do not contribute Si into the environment). Groundwater samples from the Psachna Basin

present a wide range of Si, from 4069 µg/L to 41954 µg/L, with a median value of 15616 µg/L. Circulating groundwater dissolves Si derived from chemical weathering of silicate minerals in rocks and sediments (Hem 1985), and its content in groundwater is directly proportional to its residence time, because prolonged contact with silicate rocks increases Si concentration (Khan et al. 2015). Therefore,

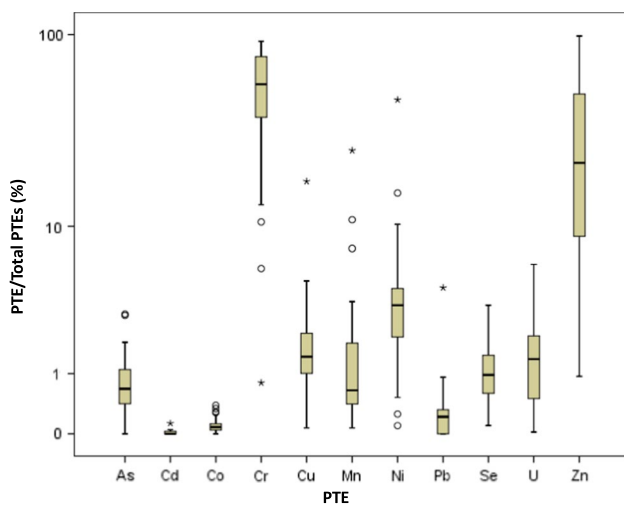


Fig. 5 The variation of the percentage of each PTE of the Psachna Basin.

high concentrations of dissolved Si may indicate extensive dissolution of silicate minerals in groundwater (Lee and Gilkes 2005). Most modern hydrogeochemical studies neglect to determine the concentration of dissolved Si in water samples for analysis. However, as shown in this work, the determination of dissolved Si could provide important information. Furthermore, Si is an element derived from silicate minerals, which are important hosts for PTEs. Calculation of an ionic ratio containing Si could provide interesting information about the geochemistry of PTEs. In addition, many studies misuse geochemical modeling without considering the silicate mineral phases, because there is no Si analysis in aqueous solutions. Such an approach neglects the largest and most important part of the geological and geochemical environment related to water chemistry, leading to misleading results.

Delignating the origin of PTEs in groundwater based on a four-step novel approach

Various approaches have been used to evaluate the origin of chemical substances in the environment. Multivariate statistical analyses (e.g., Papazotos et al. 2020; Vasileiou et al. 2019), multi-isotopic approaches (e.g., Puig et al. 2017), and machine learning algorithms (Ruidas et al. 2021; Ruidas et al. 2022) have been widely used in modern hydrogeochemical studies; the main objective has been to further investigate the complex isotopic signatures and their fractionation or to reveal the hidden geochemical relationships between chemical variables to assign natural and anthropogenic influences. Here, for the first time a four-step method is presented (Fig. 6) that combines statistics and molar ratios of specific chemical components (i.e., NO_3^- , Si,

Cl^- , and HCO_3^-) to distinguish geogenic and anthropogenic contributions of PTEs in groundwater and provide answers to the hot research topic of their occurrence, transport, and fate in the environment (Papazotos 2021). The approach is applied in the ultramafic-dominated area of the Psachna Basin, a coastal area containing rocks enriched in PTEs and characterised by intense anthropogenic pressures.

Step 1: Data collection and target a parameter

This phase includes the data collection that will be used in the next steps of the methodology. The data could come from a new sampling campaign that includes the determination of chemical parameters or a detailed literature search. For the proposed approach, only the specific chemical parameters NO_3^- , Cl^- , HCO_3^- and Si (or SiO_2) need to be determined. Here, six PTEs (i.e., As, Cr, Ni, Se, U, and Zn) were selected as target parameters to determine their origin in the Psachna Basin.

Step 2: Classification

In this step, information is categorized according to the target parameter's concentration. There are various methods of categorization that can be used. The use of guideline values for safe drinking water by the World Health Organization (WHO) or the limited values mandated by individual countries' laws can lead to inequitable groups that do not adequately represent the full range of PTEs concentrations in water resources. Since most PTEs are not mobilized in the typically encountered pH range of groundwater, it is critical to investigate concentrations below the guideline values for drinking water defined by WHO. Consequently, it is highly recommended to classify the analyzed parameters using descriptive statistics. In particular, the quartiles allow to divide the entire range of values into four approximately equal groups separated by concentration. In this work, the data shown in Table 2 were used to divide the PTEs into different categories.

Step 3: Creating hydrogeochemical diagrams

This phase involves the calculation and plotting of challenging molar ratios to investigate the hydrogeochemical footprint of specific geogenic or anthropogenic influences. Hydrochemical salinization was studied using the molar ratio of $\text{Cl}^-/\text{HCO}_3^-$; values from 1.3 to 2.8 indicate a moderate salinization effect; values < 0.5 indicate no salinization effect; values between 0.5 and 1.3 indicate a slight effect, between 2.8 and 6.6 indicate a strong salinization effect, and values > 6.6 can be interpreted as a strong salinization effect (Revelle 1941). The dominance of the anion HCO_3^- over Cl^- is indicative of recharge water and dissolution of carbonate.

Fig. 6 A four-step methodology to identify the origin of a selected chemical parameter in groundwater.

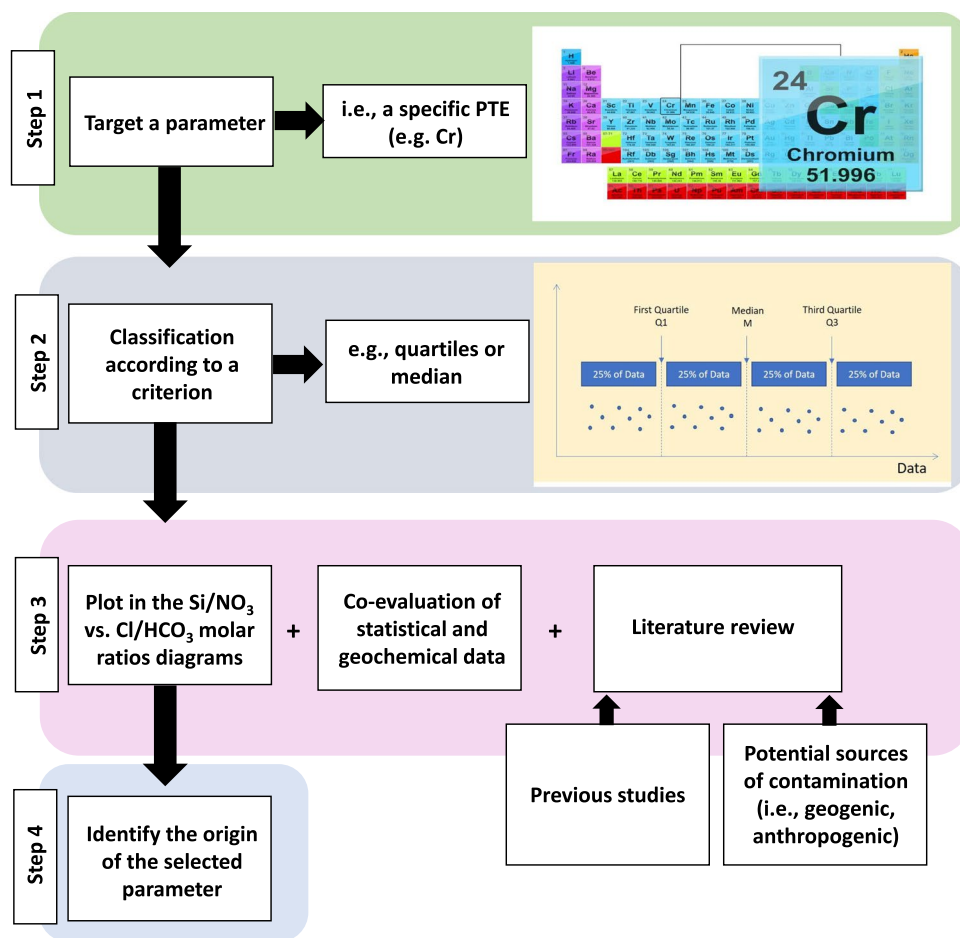


Figure 7 shows that most samples from the Psachna Basin are plotted in the "carbonate dissolution" field, indicating that groundwater recharge is a dominant hydrogeologic process. However, some samples have a Cl/HCO_3 molar ratio > 1 , indicating the influence of saltwater intrusion occurring in part of the Psachna Basin, as indicated by many researchers (Papazotos et al. 2019; Remoundaki et al. 2016). In general, seawater has very high Cl concentrations; a typical range is 17000–23000 mg/L and generally low HCO_3 concentrations (usually between 130 mg/L and 180 mg/L) with extremely high Cl/HCO_3 ratio values (> 200).

For the first time, an alternative molar ratio was used to determine whether water-rock interaction or fertilization was a major contributor to groundwater contamination. The Si/NO_3 molar ratio was evaluated, and it is crucial to investigate the range of values of ordinary aqueous solutions (such as rainwater and seawater), which are used as reference values and provide valuable hidden features of this work. In general, the concentrations of Si and NO_3^- in seawater and rainwater are very low. However, typical Si concentrations in seawater vary from 1 mg/L to 5 mg/L, and NO_3^- ranges from 0.02 mg/L to 2 mg/L, suggesting a very high Si/NO_3 molar ratio values that in most cases exceed the value of 100 (i.e.,

when anthropogenic activities that create high NO_3^- concentrations are absent) and indicating the natural origin of these aqueous solutions. The < 1 molar ratio values indicate that there is evidence of significant NO_3 loading from various N-rich sources (such as N-containing or mixed fertilizers, sewage effluents, and septic tanks); the > 2.2 values indicate a significant contribution of siliceous mineral phases to the water-rock interaction. The value of 2.2 was obtained from a common sample unaffected by anthropogenic activities ($\text{NO}_3^- = 5$ mg/L; Kim et al. 2015) and a relatively low dissolved Si concentration ($\text{Si} = 5$ mg/L; the median value for dissolved Si in this dataset from the Psachna Basin is 15.6 mg/L). In any case, the molar ratio should be evaluated concerning the geochemical conditions, the examination of the principles of Si- and N- geochemistry, and the assessment of the existing dataset. Figure 8 shows that most of the Psachna Basin samples are plotted in the "nitrate pollution" field, presenting a Si/NO_3 molar ratio < 1 . Nevertheless, some samples have a Si/NO_3 molar ratio > 1 , shown in the "Silicate dissolution" box, illustrating the influence of geology on groundwater chemistry. In any case, the coexistence of geogenic (i.e., water-rock/soil interaction) and anthropogenic (i.e., agricultural activities, sewage effluents, etc.)

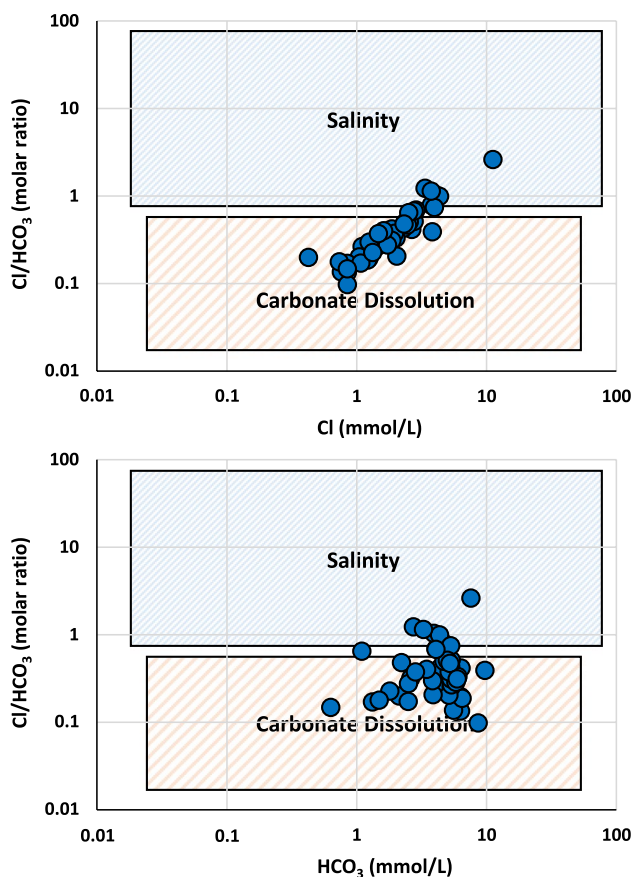


Fig. 7 The Cl/HCO₃ (molar ratio) vs. Cl (in mmol/L) and the Cl/HCO₃ (molar ratio) vs. HCO₃ (in mmol/L) diagrams contain carbonate dissolution and salinity fields of the Psachna Basin.

factors cannot be ruled out, but this should be investigated by evaluating the entire data.

It should be noted that element’s concentration is always an important indicator for environmental research and should be taken into account, since negligible data could lead to misleading results and the one-sided study of molar ratios does not give the scientist the desired result. For example, areas relatively unaffected by human activities usually have NO₃⁻ concentrations of less than 10 mg/L (Panno et al. 2006); therefore, concentrations below 0.16 mmol/L NO₃⁻ should not be attributed to anthropogenic activities, regardless of the Si/NO₃ molar ratio. On the other hand, a high to very high Si/NO₃ molar ratio followed by low Si concentrations should not be attributed to dissolution of silicates, but to other natural factors (i.e., dissolution of another predominant rock type such as carbonates, seawater, rainwater, etc.).

Finally, the combination of the two molar ratios (Cl/HCO₃ vs. Si/NO₃) provides interesting information about the groundwater chemistry of a complex aquifer system considering saltwater intrusion, agricultural activities, and water-rock interaction (including both carbonate and silicate

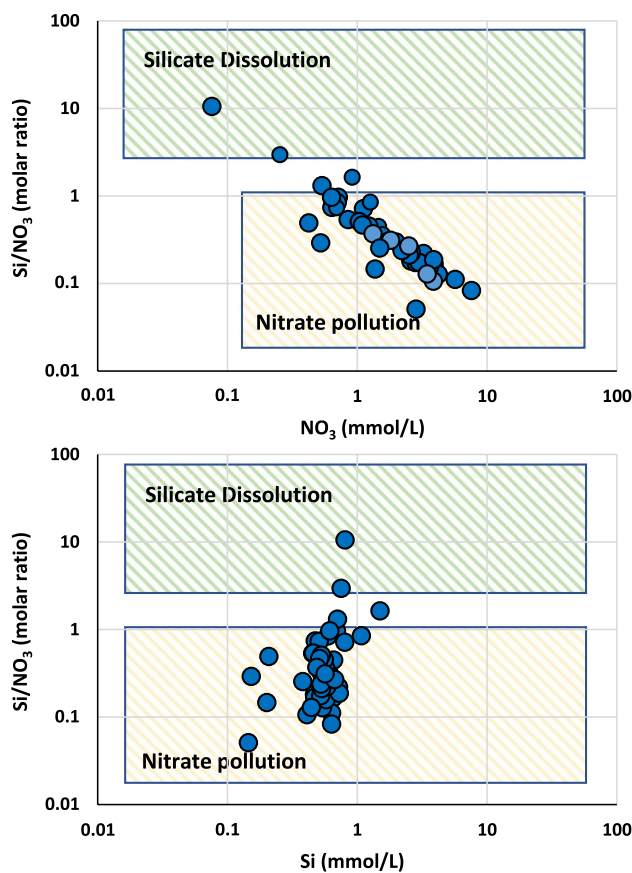


Fig. 8 The Si/NO₃ (molar ratio) vs. NO₃ (in mmol/L) and the Si/NO₃ (molar ratio) vs. Si (in mmol/L) diagrams contain silicate dissolution and nitrate pollution fields.

mineral phases) (Fig. 9). Step 3 of the present approach also contains the exhaustive co-evaluation of statistical and geochemical data and a thorough literature review, mainly focusing on previous studies from the study area and recording

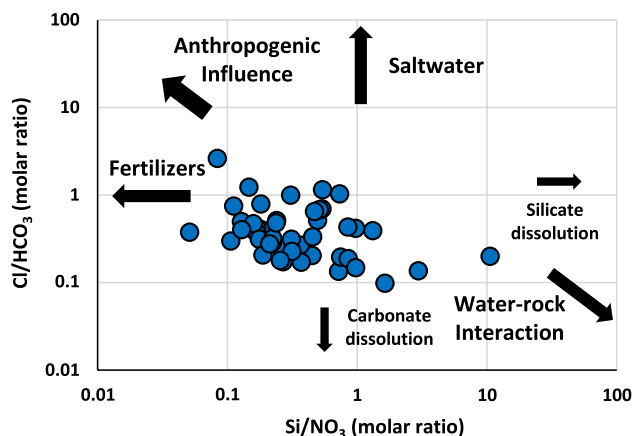


Fig. 9 Evaluation of major hydrogeochemical processes affecting water chemistry using Cl/HCO₃ vs. Si/NO₃ diagram.

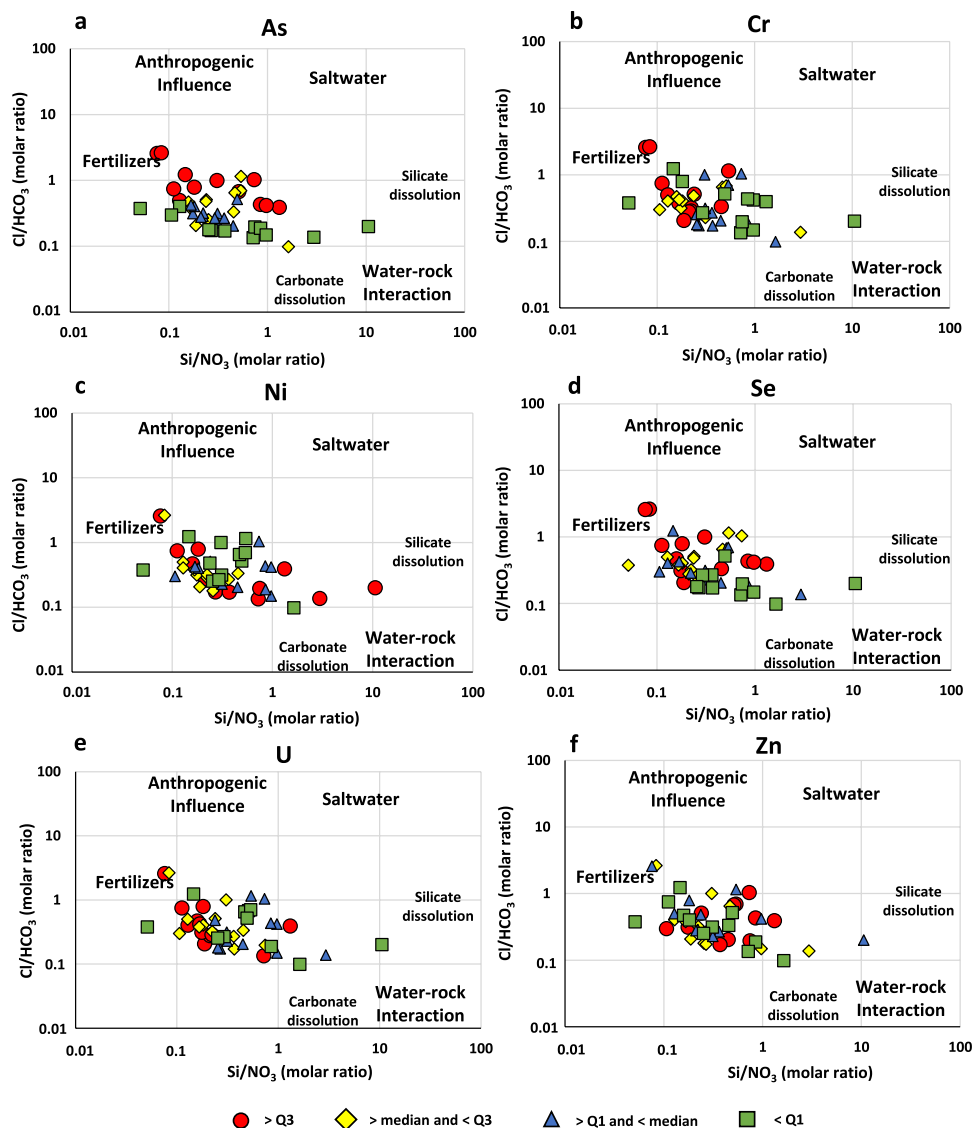
both geogenic and anthropogenic contamination sources in the environment.

Step 4: Determine the origin of PTE

After completing steps 1 to 3, the researcher is able to generate complex diagrams showing where the PTEs in the groundwater come from; in this case, the methodology is applied to As, Cr, Ni, Se, U, and Zn, and the results are shown in Fig. 10. The high salinity caused by saltwater intrusion in some areas of the Psachna Basin is responsible for the elevated As concentration in groundwater, as shown by the correlation between As concentration and Cl/HCO_3 ratio (Fig. 10a). The R-mode HCA and Spearman's rank correlation coefficients, which highlight the statistical correlation with parameters that have elevated concentrations in seawater, such as Cl^- , Br^- , and Li , further support this

hypothesis. Megremi et al. (2019) mentioned that As and Li are chemical parameters influenced by saltwater intrusion in the Psachna Basin, and modern literature confirms the role of saltwater intrusion in As mobilization (Papazotos et al. 2020). The oxidizing geochemical environment, which favors the stable presence of NO_3^- in groundwater and inhibits As desorption from Fe/Mn oxyhydroxides from rocks and soils into the aquifer, is responsible for the low groundwater concentrations of As (up to 3.3 g/L) (Guo et al. 2014). Normally, oxidative environments prevent reductive dissolution of Fe/Mn oxyhydroxides, resulting in high groundwater concentrations of NO_3^- (Xie et al. 2008). Compared to As, Cr shows a distinct pattern in the Cl/HCO_3 vs. Si/NO_3 plot (Fig. 10b). The class with the highest concentrations ($> Q_3$), indicating agricultural activities as the main contributor to Cr, is entirely dominated by low values of the Si/NO_3 ratio. Although Cr concentrations of up to 130 $\mu g/L$ have

Fig. 10 Bivariate Cl/HCO_3 vs. Si/NO_3 diagrams of a) As, b) Cr, c) Ni, d) Se, e) U, and f) Zn.



been recorded and are due to the geogenic background of an ultramafic area (Vasileiou et al. 2021), the synergistic role of agricultural activities has been shown to increase groundwater concentrations of Cr in an ultramafic environment (Papazotos et al. 2019; Vasileiou et al. 2019). This was particularly evident in the agricultural-dominant Psachna Basin, where nitrogen (N) and phosphorus (P)-containing fertilizers were widely applied (Papazotos et al. 2019). The strong positive, statistically significant correlation coefficients between Cr and NO_3^- ($r=0.66$) consistently observed over time in the study area (Vasileiou et al. 2014; Megremi et al. 2019, Papazotos et al. 2019, Remoundaki et al. 2016), and the R-mode HCA provide additional evidence of the role of fertilization (Fig. 2). Finally, Table 5 shows four different wells sampled at different times. As shown in Table 5, there is a simultaneous decrease or increase in the chemical parameters of NO_3^- and Cr. Both the chemical parameters of NO_3^- and Cr decrease or increase simultaneously, as shown in Table 5. Therefore, one chemical parameter (i.e., NO_3^-) must be the cause and the other chemical parameter must be the causal effect, implying a spatiotemporal dependence (i.e., Cr).

The proximity of Cr to other chemical parameters such as U, Si, HCO_3^- , and Ni was also revealed by a rescaled approach for R-mode HCA. Especially, Ni shows a scattering of elevated concentrations in the Cl/HCO_3^- vs. Si/NO_3^- plot (Fig. 10c). However, the samples with the lowest Cl/HCO_3^- ratio appear to have the highest Ni concentrations, suggesting that water-rock interaction is the main factor for elevated Ni concentrations. It is common for Ni to be incorporated into the lattice structure of the silicate mineral phases that make up ultramafic rocks (e.g., Ni-bearing forsterite and chlorite). However, Ni is strongly absorbed under the prevailing alkaline pH conditions, which affects its mobilization in groundwater. The trend of increasing concentrations of Se (Fig. 10d) and U (Fig. 10e) shows similar patterns to

As and Cr, respectively. Selenium is an oxyanion-forming trace element with similar hydrogeochemical properties to As, which is fully confirmed by other studies conducted in Greece (Papazotos et al. 2020). In addition, the recent literature mentions the groundwater concentration of Se in seawater (Papazotos et al. 2020) and especially in the case of the Psachna Basin (Eliopoulos et al. 2020); a hypothesis that also emerges from the analysis of the present study through the Cl/HCO_3^- vs. Si/NO_3^- diagram, the correlation analysis of the hydrochemical parameters and the R-mode HCA. The highest U concentrations are associated with the lowest Si/NO_3^- ratio (Fig. 10e), indicating the role of fertilization on U concentrations in groundwater. In general, P-containing fertilizers cause a significant increase in U in groundwater at low concentrations (Liesch et al. 2015). As mentioned earlier, the Psachna basin is an area of intensive agricultural activities where extensive application of P-containing fertilizers has been detected (Papazotos et al. 2019). In addition, strong to very strong statistically significant correlation coefficients of $\text{U}-\text{SO}_4^{2-}$ ($r=0.796$), $\text{U}-\text{NO}_3^-$ (0.625), and $\text{U}-\text{Ca}^{2+}$ ($r=0.863$) demonstrate that the main source of U in groundwater is the fertilizers used in this area. The high concentrations of SO_4^{2-} and NO_3^- were attributed to the fertilizers in the Basin from previous researchers (e.g., Papazotos et al. 2019; Remoundaki et al. 2016). Fertilizers rich in phosphorus (P) are extracted from phosphate rocks that typically contain apatite-group minerals [$\text{Ca}_5(\text{PO}_4)_3(\text{F}, \text{OH})$ or Cl] and have a high Ca content; phosphate rocks are enriched in PTEs (Kratz et al. 2016; Molina et al. 2009; Papazotos et al. 2019). Psachna Basin local fertilizer market sales of P-containing fertilizers were found to have a very high PTE content, as demonstrated by Papazotos et al. (2019). Very high U content (30–200 mg/kg) can be observed in rock phosphate, in which the U substitutes for Ca^{2+} in the apatite crystal structure (Liesch et al. 2015). Strong correlations between Ca^{2+} and PTEs have been observed in other areas of Greece (e.g., Schinos area, Papazotos et al. 2020) and attributed to P-bearing fertilizers. Moreover, Zn does not show an obvious trend of the influence of the primary factors shown in the Cl/HCO_3^- vs. Si/NO_3^- plot (Fig. 10f), and therefore the origin of Zn should be sought in other causes such as the prevailing geochemical conditions (i.e., pH, Eh, D.O., etc.) and other anthropogenic factors. Under oxidizing conditions and especially at acidic to neutral pH, Zn is one of the most mobile water migrants (Alloway 2013). On the other hand, Zn precipitates under reducing conditions. In addition, it can co-precipitate with Fe/Mn oxyhydroxides in systems with high pollution if it is present in very high groundwater concentrations (Smith 1995). As a result, Fe/Mn oxyhydroxides, clay minerals, and organic matter in waters readily bind to Zn and form organometallic complexes that increase the ionic strength of the solution (Diatla and Kociałkowski, 1998). Sorption of Zn increases with

Table 5 NO_3^- and Cr groundwater concentrations and their percentage variability from selected wells sampled at different periods.

Well number	Sampling period	NO_3^- mg/L	Cr μg/L	ΔNO_3^- (%)	ΔCr (%)
1	June 2017	96.9	57.7	-59.3	-51.5
	November 2017	39.4	28		
2	December 2016	43.3	36.5	1.85	12.6
	June 2017	44.1	41.1		
2	June 2017	44.1	41.1	-24.9	-69.3
	November 2017	33.1	12.6		
3	December 2016	43.3	36.5	21	99.7
	November 2017	52.4	72.9		
4	June 2017	189	79.8	-8.47	-6.02
	November 2017	173	75		

increasing pH and decreasing salinity (Huang et al. 2014). Zinc cations can be easily exchanged when competing with other PTE cations (Fonseca et al. 2011). The increase in Zn sorption is followed by a decrease in salinity, as confirmed in Fig. 10f, suggesting that this is a key parameter for Zn mobility in the groundwater. The schematic distribution of TPTEs (Fig. 11) is similar to that of Cr and Zn (Figs. 10a, 10f), as expected from their high contribution to the final calculation of TPTEs.

Nevertheless, it is worth noting that geochemical conditions are the most important parameters for understanding the occurrence, mobilization, transport, and fate of PTEs in groundwater, and the proposed successful approach was applied in an ultramafic geologic setting that produces a specific geochemical footprint in groundwater (i.e., neutral to alkaline pH conditions, elevated Cr concentrations, etc.). In

a different geologic setting (e.g., dominance of carbonate rocks, etc.) or under different geochemical conditions (e.g., acidic pH or reducing Eh conditions), it is possible that the technique would need to be modified or could not be applied with the same success. Future work focusing on the application of the methodology in different areas - on a global scale - under alternative geochemical approaches is encouraged to evaluate the above framework to investigate its in-depth effectiveness, or could provide useful modifications.

Geochemical modeling

Geochemical modeling was performed to further evaluate the thermodynamic constraints of the water-rock interaction. Figure 12 shows the mineralogical phases that contribute to the chemical elements in the aquifer via chemical

Fig. 11 Bivariate Cl/HCO₃ vs. Si/NO₃ diagram of TPTEs.

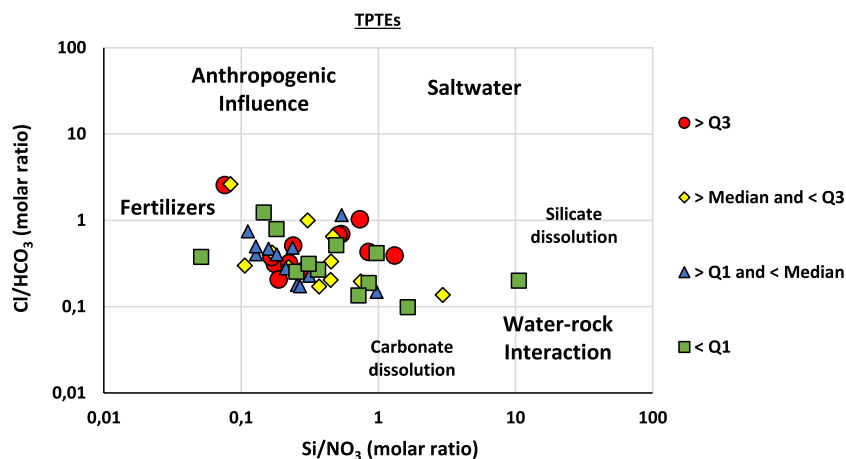
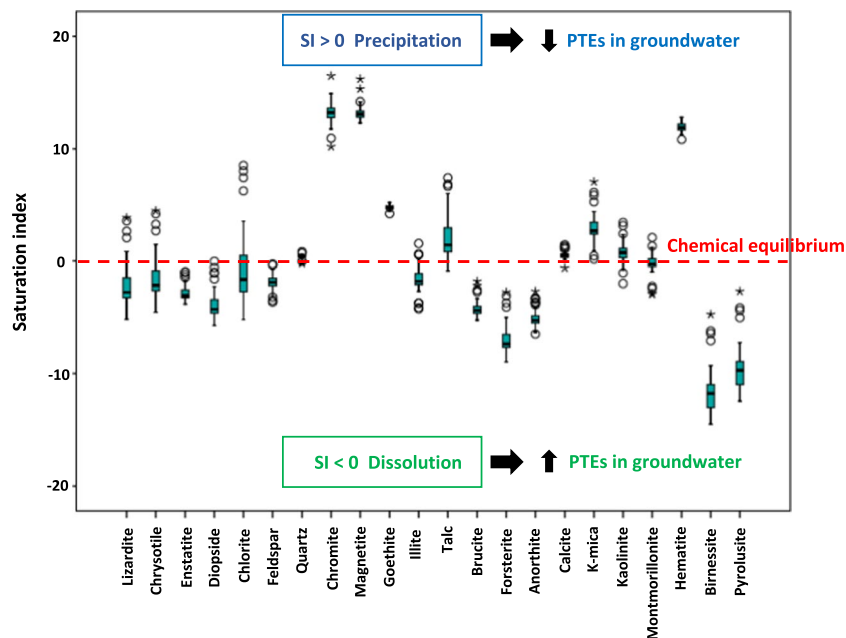


Fig. 12 Saturation indices of examined mineral phases from the Psachna Basin.



dissolution. It is important to note that the theoretically oversaturated minerals do not contribute elements to the water due to the prevailing geochemical conditions.

The conceptual model of the potential dissolution/precipitation mechanism is shown in Fig. 12. However, the identified mineralogical phases do not include some PTEs contained in their lattice structure. Therefore, it is very interesting to examine the Spearman correlation coefficients with selected PTEs (Table 6) to draw meaningful conclusions about the contribution of chemical thermodynamics to environmental geochemistry. Most of the results show negative correlations, proving that PTEs in groundwater are caused by mineral dissolution. Because these are theoretical calculations based largely on the chemistry of major ions and selected PTEs, strong to very strong correlation coefficients are not expected to be found. If this hypothesis were true, it would be reflected primarily in the table of correlation coefficients for all parameters (see Table 3). The saturation index for chromite was calculated using Cr, so there is a positive correlation between the two variables ($r=0.522$; $p=0.01$). Nonetheless, statistically significant correlations are evident and need to be further investigated in future work. Targeted future research on the thermodynamic characteristics of the PTE-containing mineralogical phases and a thorough geochemical modeling study (including

forward and inverse modeling techniques) on their dissolution reactions and environmental footprint could provide very interesting insights to the geoscience community. This would undoubtedly be a significant step forward in research related to PTE and would help researchers better understand the many unanswered questions.

Conclusions

For more than ten years, the quality of groundwater in the Psachna Basin in central Euboea, Greece, has been studied in detail. A methodology to distinguish geogenic and anthropogenic influences controlling the geochemistry of PTE using ionic ratios (i.e. Si/NO_3 and Cl/HCO_3). For the first time, sophisticated ion ratios have been combined to produce hydrogeochemical diagrams showing the origin of each PTE in groundwater resources. The novel methodology was successfully applied in the Psachna Basin, and the analysis revealed that significant groundwater contamination originated mainly from water-rock interaction, over-fertilization, and saltwater intrusion. The main advantages of the proposed methodology are that it is easy to apply, as in the case of the successful application in the ultramafic study area mentioned above, and that it

Table 6 Spearman rank correlation matrix and correlation significance (p values) of selected PTEs and the SIs of examined mineral phases of the groundwater samples of the Psachna Basin (N = 47). Color represents the classification of the absolute correlation value between two parameters i.e., Yellow: 0.40-0.59, Blue: 0.20-0.39, and Green: 0.00-0.19.

Mineral Phase	As	Co	Cr	Cu	Mn	Ni	Se	U	Zn
Lizardite	-0.169	-0.007	0.069	-0.034	-0.014	-0.255	-0.157	-0.367*	-0.086
Chrysotile	-0.169	-0.007	0.069	-0.034	-0.014	-0.255	-0.157	-0.367*	-0.086
Enstatite	-0.166	0.064	0.123	0.016	0.018	-0.193	-0.111	-0.316*	-0.100
Diopside	-0.161	0.029	0.114	-0.007	0.002	-0.230	-0.134	-0.310*	-0.076
Chlorite	-0.247	0.099	0.134	0.018	0.001	-0.152	-0.171	-0.301*	-0.082
Feldspar	0.102	0.336*	0.389**	0.274	0.147	0.251	0.133	0.065	-0.046
Quartz	0.125	0.270	0.185	0.159	-0.011	0.429**	0.151	0.154	-0.116
Chromite	0.102	0.185	0.522**	0.214	0.166	0.039	0.077	-0.090	0.062
Magnetite	-0.037	-0.259	-0.102	0.058	-0.100	-0.113	-0.214	-0.341*	0.069
Goethite	-0.304*	-0.246	-0.180	-0.206	-0.160	-0.436**	-0.387**	-0.557**	-0.073
Illite	0.037	0.412**	0.381**	0.244	0.157	0.387**	0.193	0.286	-0.040
Talc	-0.168	0.105	0.146	0.037	0.054	-0.142	-0.083	-0.267	-0.099
Brucite	-0.205	-0.093	-0.028	-0.110	-0.087	-0.343*	-0.240	-0.444**	-0.076
Forsterite	-0.174	-0.049	0.038	-0.067	-0.030	-0.294*	-0.184	-0.399**	-0.083
Anorthite	-0.123	0.339*	0.334*	0.198	0.068	0.280	0.077	0.302*	0.059
Calcite	-0.265	-0.093	-0.051	-0.107	-0.097	-0.260	-0.208	-0.130	0.051
K_mica	0.068	0.430**	0.398**	0.277	0.180	0.412**	0.230	0.336*	-0.011
Kaolinite	0.076	0.341*	0.323*	0.187	0.078	0.438**	0.251	0.426**	-0.020
Montmorillonite	-0.078	0.360*	0.296*	0.170	0.084	0.394**	0.110	0.279	-0.051
Hematite	-0.300*	-0.243	-0.181	-0.209	-0.165	-0.434**	-0.386**	-0.556**	-0.075
Birnessite	-0.062	-0.030	0.080	-0.188	0.142	-0.276	-0.045	-0.100	0.124
Pyrolusite	-0.060	-0.034	0.079	-0.191	0.142	-0.276	-0.045	-0.103	0.127

** . Correlation is significant at the 0.01 level (2-tailed).

* . Correlation is significant at the 0.05 level (2-tailed).

could be implemented in any geological setting with minor modifications due to its flexible methodological framework (e.g., different data classification methods), providing insight to the (geo)scientific community. Primarily, high groundwater concentrations of Cr that systematically exceed the guideline values of WHO (i.e., 50 µg/L) are attributed to intensive agricultural activities, a hypothesis consistent with many other researchers. Lower, but by no means negligible, concentrations of U are also attributed to P-containing fertilizers. On the other hand, the methodology described in this study revealed that the occurrence and mobility of As, Se, and Zn in groundwater are related to saltwater intrusion. Finally, Ni seems to be mainly related to geogenic factors, although its occurrence is significantly controlled by the prevailing geochemistry, a key factor whose influence cannot be ignored in the analysis of PTE. In addition, the use of real mineralogical data in geochemical modeling studies underscores the need for detailed interdisciplinary studies of hydrogeochemistry, which contribute significantly to a better understanding of the potential contribution of water-rock interactions to the groundwater system. This analysis shows that many silicate mineral phases are undersaturated in an aqueous solution (i.e., groundwater), suggesting a potential contribution from PTEs (and other major/minor elements). This initial approach to the important issue of PTEs in water resources through Si/NO₃ vs. Cl/HCO₃ diagrams can be a useful methodological framework to describe the origin of PTEs in groundwater, especially if this approach is combined with the use of advanced statistical methods (i.e., PCA, HCA, etc.), geospatial data analysis, multi-isotope approaches, and machine learning algorithms allows for a holistic assessment of a complex and challenging topic such as the origin, occurrence, mobilization, transport, and fate of PTEs in the environment and, in particular, in a sensitive receptor such as water resources.

There are two major limitations to the above proposed methodology:

(a) the determination of certain chemical parameters, such as NO₃⁻, Cl⁻, HCO₃⁻, and Si, is required because these data are mandatory for the proposed method; and (b) the limited thermodynamic data, since the thermodynamic geochemical databases (e.g., PHREEQC, MINTEQA, etc.) do not include the formulas of the PTE-bearing mineralogical phases, neglecting that many PTEs are included in their lattice structure; this fact must be taken into account, otherwise researchers will not be able to fully understand the geogenic system and will therefore obtain misleading results regarding complex water-rock-soil interaction processes.

The implications of this research are expected to be significant to the scientific community still seeking answers to the complex question of the origin of PTEs in groundwater, as it allows researchers to apply a specific methodology to

further investigate their data set in the context of advanced environmental geochemistry. Specifically, this work aims to develop a holistic methodology that can be (a) applied globally and in any geological setting, and (b) applied by researchers, making a critical contribution to the scientific community's understanding of the occurrence, mobilization, and geochemistry of PTEs and achieving breakthroughs in environmental science and pollution research. The results of this study will be applied by environmental scientists to create a powerful tool for understanding the origin of PTEs and contribute to a new regulatory framework that enhances both environmental awareness and human health.

Acknowledgements The authors would like to thank the three anonymous reviewers for their constructive remarks and recommendations, which greatly improved the quality of the present paper. Special thanks are extended to the editor, Dr. Xianliang Yi, for his careful editing handling.

Authors Contributions PP: conceptualization, formal analysis, methodology, data curation, writing—original draft, writing—review and editing, project administration, review and editing, visualization, investigation. EV: formal analysis, data curation, validation, writing—review and editing, investigation. SV: data curation, formal analysis, writing—review and editing, investigation. MP: validation, data curation, writing—review and editing, project administration, supervision. All authors read and approved the final manuscript.

Funding This research was funded by the NTUA research committee.

Data availability Data will be made available on request.

Declarations

Ethical Approval Not applicable.

Consent to Participate Not applicable.

Consent to Publish Not applicable.

Competing Interests The author declares no competing interests.

References

- Abdalla F (2016) Ionic ratios as tracers to assess seawater intrusion and to identify salinity sources in Jazan coastal aquifer, Saudi Arabia, *Arab J Geos.* 1–12. doi: <https://doi.org/10.1007/s12517-015-2065-3>
- Alcalá FJ, Custodio E (2008) Using the Cl/Br ratio as a tracer to identify the origin of salinity in aquifers in Spain and Portugal. *J Hydrol* 359. doi: <https://doi.org/10.1016/j.jhydrol.2008.06.028>
- Allison JD, Brown DS, Novo-Gradac KJ (1991) MInteqa2/Prodefa2, a Geochemical Assessment Model for Environmental Systems: Version 3.0 User'S Manual. U. S. Environ. Prot. Agency EPA/600/3-91/021
- American Public Health Association (APHA) (2012) Standard Methods for the Examination of Water and Wastewater, 27th Ed. Washington, DC
- Ball JW, McCleskey RB (2003) A new cation-exchange method for accurate field speciation of hexavalent chromium. *Talanta* 61:. doi: [https://doi.org/10.1016/S0039-9140\(03\)00282-0](https://doi.org/10.1016/S0039-9140(03)00282-0)

- Chen F, Jia G, Chen J (2009) Nitrate sources and watershed denitrification inferred from nitrate dual isotopes in the Beiji River, south China. *Biogeochem* 94. doi: <https://doi.org/10.1007/s10533-009-9316-x>
- Diatta J, Kociałkowski W (1998) Adsorption of zinc in some selected soils. *Polish J Environ Stud* 7
- Dandolos H, Zorapas B (2010) Recording and assessment of the underground aquifer systems of Boeotian Kifissos and the sub-selected prefecture of Viotia - Evia. Athens: Institute of Geological and Mining Exploration (in Greek)
- Economou-Eliopoulos M, Frei R, Atsarou C (2014) Application of chromium stable isotopes to the evaluation of Cr(VI) contamination in groundwater and rock leachates from central Euboea and the Assopos basin (Greece). *Catena* 122:216–228. <https://doi.org/10.1016/j.catena.2014.06.013>
- Economou-Eliopoulos M, Megremi I, Vasilatos C et al (2017) Geochemical constraints on the sources of Cr(VI) contamination in waters of Messapia (Central Evia) Basin. *Appl Geochemistry* 84:13–25. <https://doi.org/10.1016/j.apgeochem.2017.05.015>
- Egbueri, JC, Agbasi, JC (2022) Combining data-intelligent algorithms for the assessment and predictive modeling of groundwater resources quality in parts of southeastern Nigeria. *Environ Sci Pollut Res*. doi: <https://doi.org/10.1007/s11356-022-19818-3>
- Eliopoulos GD, Eliopoulos IPD, Tsioubri M, Economou-Eliopoulos M (2020) Distribution of selenium in the soil–plant–groundwater system: Factors controlling its bio-accumulation. *Minerals* 10. doi: <https://doi.org/10.3390/min10090795>
- Eliopoulos IPD, Eliopoulos GD, Economou-Eliopoulos M (2021) The cr(Vi) stability in contaminated coastal groundwater: Salinity as a driving force. *Minerals* 11
- Evans JD (1996) Straightforward statistics for the behavioral sciences. Thomson Brooks/Cole Publishing Co, Belmont
- Fendorf SE, Fendorf M, Sparks DL, Gronsky R (1992) Inhibitory mechanisms of Cr(III) oxidation by δ -MnO₂. *J Colloid Interface Sci* 153. doi: [https://doi.org/10.1016/0021-9797\(92\)90296-X](https://doi.org/10.1016/0021-9797(92)90296-X)
- Filzmoser P, Hron K, Templ M (2018) Applied compositional data analysis with worked examples in R. Springer, New York
- Fonseca B, Figueiredo H, Rodrigues J, et al (2011) Mobility of Cr, Pb, Cd, Cu and Zn in a loamy sand soil: A comparative study. *Geoderma* 164. doi: <https://doi.org/10.1016/j.geoderma.2011.06.016>
- Guo H, Wen D, Liu Z, et al (2014) A review of high arsenic groundwater in Mainland and Taiwan, China: Distribution, characteristics and geochemical processes. *Appl. Geochemistry* 41
- Hem JD (1985) Study and interpretation of the chemical characteristics of natural water. US Geol Surv Water-Supply Pap 2254
- Hermann R, Neumann-Mahlkau P (1985) The mobility of zinc, cadmium, copper, lead, iron and arsenic in ground water as a function of redox potential and pH. *Sci Total Environ* 43. doi: [https://doi.org/10.1016/0048-9697\(85\)90027-0](https://doi.org/10.1016/0048-9697(85)90027-0)
- Huang B, Li Z, Huang J, et al (2014) Adsorption characteristics of Cu and Zn onto various size fractions of aggregates from red paddy soil. *J Hazard Mater* 264. doi: <https://doi.org/10.1016/j.jhazmat.2013.10.074>
- Katsikatsos G, Koukis G, Fytikas M, Anastopoulos J, Kanaris J (1981) Geological map of Greece, scale 1: 50,000, Psachna-Pilion sheet. Greek Institute of Geology and Mineral Exploration, Rethymno
- Kelepertzis E, Galanos E, Mitsis I (2013) Origin, mineral speciation and geochemical baseline mapping of Ni and Cr in agricultural topsoils of Thiva Valley (central Greece). *J Geochemical Explor* 125. doi: <https://doi.org/10.1016/j.gexplo.2012.11.007>
- Kim KH, Yun ST, Kim HK, Kim JW (2015) Determination of natural backgrounds and thresholds of nitrate in South Korean groundwater using model-based statistical approaches. *J Geochemical Explor* 148. <https://doi.org/10.1016/j.gexplo.2014.10.001>
- Khan A, Umar R, Khan HH (2015) Significance of silica in identifying the processes affecting groundwater chemistry in parts of Kali watershed, Central Ganga Plain, India. *Appl Water Sci* 5. doi: <https://doi.org/10.1007/s13201-014-0164-z>
- Köppen W (1931) Grundriss der Klimakunde. (Zweite, verbesserte Auflage der Klimate der Erde.) Walter de Gruyter & Co., Berlin, Leipzig, 388 pp.
- Kotaś J, Stasicka Z (2000) Chromium occurrence in the environment and methods of its speciation. *Environ Pollut* 107:263–283. [https://doi.org/10.1016/S0269-7491\(99\)00168-2](https://doi.org/10.1016/S0269-7491(99)00168-2)
- Kratz S, Schick J, Schnug E (2016) Trace elements in rock phosphates and P containing mineral and organo-mineral fertilizers sold in Germany. *Sci Total Environ* 542. doi: <https://doi.org/10.1016/j.scitotenv.2015.08.046>
- Lee SY, Gilkes RJ (2005) Groundwater geochemistry and composition of hardpans in southwestern Australian regolith. *Geoderma* 126. doi: <https://doi.org/10.1016/j.geoderma.2004.11.007>
- Liesch T, Hinrichsen S, Goldscheider N (2015) Uranium in groundwater - Fertilizers versus geogenic sources. *Sci Total Environ* 536. doi: <https://doi.org/10.1016/j.scitotenv.2015.05.133>
- Małeckii JJ, Kadzikiewicz-Schoeneich M, Eckstein Y, et al (2017) Mobility of copper and zinc in near-surface groundwater as a function of the hypergenic zone lithology at the Kampinos National Park (Central Poland). *Environ Earth Sci* 76. doi: <https://doi.org/10.1007/s12665-017-6527-7>
- Megremi, I. (2010). Controlling factors of the mobility and bioavailability of Cr and other metals at the environment of Ni-Laterites. Ph.D thesis. University of Athens
- Megremi I, Vasilatos C, Vassilakis E, Economou-Eliopoulos M (2019) Spatial diversity of Cr distribution in soil and groundwater sites in relation with land use management in a Mediterranean region: The case of C. Evia and Assopos-Thiva Basins, Greece. *Sci Total Environ* 651. doi: <https://doi.org/10.1016/j.scitotenv.2018.09.186>
- Mills CT, Goldhaber MB (2012) Laboratory investigations of the effects of nitrification-induced acidification on Cr cycling in vadose zone material partially derived from ultramafic rocks. *Sci Total Environ* 435–436. doi: <https://doi.org/10.1016/j.scitotenv.2012.06.054>
- Molina M, Aburto F, Calderón R et al (2009) Trace element composition of selected fertilizers used in Chile: Phosphorus fertilizers as a source of long-term soil contamination. *Soil Sediment Contam* 18. <https://doi.org/10.1080/15320380902962320>
- Oze C, Fendorf S, Bird DK, Coleman RG (2004) Chromium geochemistry in serpentinized ultramafic rocks and serpentine soils from the Franciscan complex of California. *Am J Sci* 304. doi: <https://doi.org/10.2475/ajs.304.1.67>
- Papazotos P (2021) Potentially toxic elements in groundwater: a hotspot research topic in environmental science and pollution research. *Environ Sci Pollut Res*. doi: <https://doi.org/10.1007/s11356-021-15533-7>
- Papazotos P, Vasileiou E, Perraki M (2020) Elevated groundwater concentrations of arsenic and chromium in ultramafic environments controlled by seawater intrusion, the nitrogen cycle, and anthropogenic activities: The case of the Gerania Mountains, NE Peloponnese, Greece. *Appl Geochemistry* 121. doi: <https://doi.org/10.1016/j.apgeochem.2020.104697>
- Papazotos P, Vasileiou E, Perraki M (2019) The synergistic role of agricultural activities in groundwater quality in ultramafic environments: the case of the Psachna basin, central Euboea, Greece. *Environ Monit Assess* 191. doi: <https://doi.org/10.1007/s10661-019-7430-3>
- Papazotos P, Vasileiou E, Perraki M (2019b) Chromium-manganese redox couple resulting in elevated Cr⁶⁺ concentration in groundwater of the Psachna basin, Central Euboea, Greece. Proceedings of the 15th International Congress of the Geological Society of Greece, Athens, May 2019
- Parkhurst DL, Appelo CAJ (1999) User's Guide to PHREEQC (Version 2): A Computer Program for Speciation, Batch-Reaction,

- One-Dimensional Transport, and Inverse Geochemical Calculations
- Pourbaix M (1966) Atlas of electrochemical equilibria in aqueous solutions (English edition). Pergamon press, Oxford.
- Puig R, Soler A, Widory D, Mas-Pla J, Domènech C, Otero N (2017) Characterizing sources and natural attenuation of nitrate contamination in the Baix Ter aquifer system (NE Spain) using a multi-isotope approach. *ci Total Environ* 518–532. doi: 10.1016/j.scitotenv.2016.11.206
- Rai D, Sass BM, Moore DA (1987) Chromium(III) Hydrolysis Constants and Solubility of Chromium(III) Hydroxide. *Inorg Chem* 26:. doi: <https://doi.org/10.1021/ic00250a002>
- Remoundaki E, Vasileiou E, Philippou A et al (2016) Groundwater Deterioration: The Simultaneous Effects of Intense Agricultural Activity and Heavy Metals in Soil. *Procedia Engineering*, In
- Revelle R (1941) Criteria for recognition of the sea water in groundwaters. *Eos, Trans Am Geophys Union* 22:. doi: <https://doi.org/10.1029/TR022i003p00593>
- Richard FC, Bourg ACM (1991) Aqueous geochemistry of chromium: A review. *Water Res* 25:. doi: [https://doi.org/10.1016/0043-1354\(91\)90160-R](https://doi.org/10.1016/0043-1354(91)90160-R)
- Ruidas D, Chakraborty R, Islam ARMT, Saha A, Pal, SC (2022) A novel hybrid of meta-optimization approach for flash flood-susceptibility assessment in a monsoon-dominated watershed, Eastern India. *Environ Earth Sci* 81:. doi: <https://doi.org/10.1007/s12665-022-10269-0>
- Ruidas D, Pal SC, Islam ARMT, Saha,A (2021) Characterization of groundwater potential zones in water-scarce hardrock regions using data driven model. *Environ Earth Sci* 80:. doi: <https://doi.org/10.1007/s12665-021-10116-8>
- Ryan PC, Kim J, Wall AJ, et al (2011) Ultramafic-derived arsenic in a fractured bedrock aquifer. *Appl Geochemistry* 26:. doi: <https://doi.org/10.1016/j.apgeochem.2011.01.004>
- Smith L (1995) Contamination and Remedial Options at Selected Metal-Contaminated Sites. *Epa/540/R-95/512*
- Spearman C (1904) The Proof and Measurement of Association between Two Things. *Am J Psychol* 15:. doi: <https://doi.org/10.2307/1412159>
- Vasilakis S, Papazotos P, Vasileiou E, Perraki M (2022). Coupling DRASTIC method and hydrogeochemical indices for the assessment of the vulnerability and the groundwater quality in the Psachna Basin, Central Euboea, Greece. 12th International Hydrogeological Congress of Greece, March 2022, Cyprus
- Vasileiou E, Papazotos P, Dimitrakopoulos D, Perraki M (2019) Expounding the origin of chromium in groundwater of the Sarigkiol basin, Western Macedonia, Greece: a cohesive statistical approach and hydrochemical study. *Environ Monit Assess* 191:. doi: <https://doi.org/10.1007/s10661-019-7655-1>
- Vasileiou E, Papazotos P, Dimitrakopoulos D, Perraki M (2021) Hydrogeochemical processes and natural background levels of chromium in an ultramafic environment. The case study of vermio mountain, western macedonia, greece. *Water (Switzerland)* 13:. doi: <https://doi.org/10.3390/w13202809>
- Vasileiou E, Perraki M, Stamatis G, Gartzos E (2014). The effects of water rock interaction and the human activities on the occurrence of hexavalent chromium in waters. The case study of the Psachna basin, central Euboea, Greece. *EGU General Assembly 2014, 27 April–2 May, 2014 in Vienna, Austria, id.15467*
- Vithanage M, Rajapaksha AU, Oze C et al (2014) Metal release from serpentine soils in Sri Lanka. *Environ Monit Assess* 186:3415–3429. <https://doi.org/10.1007/s10661-014-3626-8>
- Voutsis N, Kelepertzis E, Tziritis E, Kelepertzis A (2015) Assessing the hydrogeochemistry of groundwaters in ophiolite areas of Euboea Island, Greece, using multivariate statistical methods. *J Geochemical Explor* 159:. doi: <https://doi.org/10.1016/j.gexplo.2015.08.007>
- Ward J. (1963) Hierarchical grouping to optimize an objective function. *Journal of the American Statistical Association*, 58.
- Xie X, Wang Y, Su C, et al (2008) Arsenic mobilization in shallow aquifers of Datong Basin: Hydrochemical and mineralogical evidences. *J Geochemical Explor* 98:. doi: <https://doi.org/10.1016/j.gexplo.2008.01.002>

Publisher's note Springer Nature remains neutral with regard to jurisdictional claims in published maps and institutional affiliations.

Springer Nature or its licensor (e.g. a society or other partner) holds exclusive rights to this article under a publishing agreement with the author(s) or other rightsholder(s); author self-archiving of the accepted manuscript version of this article is solely governed by the terms of such publishing agreement and applicable law.